NANO Fe^0/ACTIVATED CARBON COMPOSITE APPLIED AS A CATALYST FOR THE OXIDATIVE DEGRADATION OF RHODAMINE B DYE

VẬT LIỆU TỔ HỢP NANO Fe^0/CARBON HOẠT TÍNH ỨNG DỤNG LÀM CHẤT XÚC TÁC PHÂN HỦY OXY HÓA THUỐC NHUỘM RHODAMINE B

Vu Minh Chau[1], Nguyen Thi Phuong[2], Vuong Thuy Trang[3], Nguyen Ba Cuong[4], Nguyen Thi Hong Phuong[3], Nguyen Thi Hoai Phuong[1,*]

DOI: https://doi.org/10.57001/huih5804.2025.299

ABSTRACT

This study uses nanoscale zero-valent iron (nZVI) and activated carbon to degrade Rhodamine B (RhB). The AC matrix modified and immobilized nZVI, which has strong reactivity, to reduce aggregation and preserve its reactivity. FTIR analysis showed that nZVI incorporation altered surface chemistry and functional groups, while elemental composition analysis showed that both nZVI and AC retained essential characteristics, making the composite suitable for pollutant adsorption and reduction. RhB degradation was tested at various beginning concentrations, catalyst doses, and reaction durations. Kinetic study showed a pseudo-second-order degradation model ($R^2 = 0.988$), indicating adsorption and surface contacts were the primary processes, rather than mass transfer. The pseudo-first-order model suited well but had a weaker correlation ($R^2 = 0.942$), indicating the prevalence of chemisorption. Over 80% degradation occurred in the first 60 minutes, then slowed to 90.52% after 120 minutes. These results demonstrate nZVI/AC's strong RhB removal effectiveness, indicating its promise as a wastewater treatment material. Optimization of operational parameters and long-term performance in real wastewater situations should be the focus of future research.

Keywords: *Nano zero-valent iron, activated carbon, Rhodamine B, oxidative degradation, advanced oxidation process.*

TÓM TẮT

Nghiên cứu này sử dụng sắt hóa trị bằng không (nZVI) ở quy mô nano và than hoạt tính để phân hủy Rhodamine B (RhB). Ma trận AC đã biến đổi và cố định nZVI, có khả năng phản ứng mạnh, để giảm sự kết tụ và duy trì khả năng phản ứng của nó. Phân tích FTIR cho thấy việc kết hợp nZVI đã làm thay đổi tính chất hóa học bề mặt và các nhóm chức năng, trong khi phân tích thành phần nguyên tố cho thấy cả nZVI và AC đều giữ lại các đặc điểm thiết yếu, khiến tổ hợp này phù hợp để hấp phụ và phân huỷ chất ô nhiễm. Sự phân hủy RhB đã được thử nghiệm ở nhiều nồng độ ban đầu, liều lượng chất xúc tác và thời gian phản ứng khác nhau. Nghiên cứu động học cho thấy mô hình phân hủy bậc hai giả ($R^2 = 0,988$), chỉ ra rằng sự hấp phụ và tiếp xúc bề mặt là các quá trình chính. Mô hình bậc nhất giả phù hợp nhưng có tương quan yếu hơn ($R^2 = 0,942$), cho thấy sự phổ biến của quá trình hấp phụ hóa học. Hơn 80% sự phân hủy xảy ra trong 60 phút đầu tiên, sau đó chậm lại còn 90,52% sau 120 phút. Những kết quả này chứng minh hiệu quả loại bỏ RhB mạnh mẽ của nZVI/AC, cho thấy triển vọng của nó như một vật liệu xử lý nước thải. Tối ưu hóa các thông số vận hành và hiệu suất dài hạn trong các tình huống nước thải thực tế nên là trọng tâm của nghiên cứu trong tương lai.

Từ khóa: *Nano sắt hóa trị không, than hoạt tính, Rhodamine B, phân hủy oxy hóa, quy trình oxy hóa nâng cao.*

[1]Joint Vietnam - Russia Tropical Science and Technology Research Center, Vietnam
[2]Institute of Chemistry and Materials, Academy of Military Science and Technology, Vietnam
[3]Hanoi University of Science and Technology, Vietnam
[4]Military Technical Academy, Vietnam
[*]Email: hoaiphuong1978@gmail.com
Received: 01/4/2025
Revised: 21/5/2025
Accepted: 28/7/2025

1. INTRODUCTION

Water pollution resulting from industrial discharges has emerged as a significant global environmental issue. Synthetic dyes, including Rhodamine B (RhB), are extensively utilized in the textile, paper, and cosmetic sectors among various pollutants. These dyes have significant persistence in aquatic settings owing to their intricate aromatic structures, rendering them resistant to natural degradation. As a result, their elimination from wastewater has garnered considerable study interest. Shumin's research established a method for eliminating NH_4^+-N and Rhodamine B from wastewater, demonstrating that enlarged anode electric biological (EAEB) attained a removal efficiency of up to 97.7% for RhB, surpassing conventional biological aerated filter (BAF) [1]. Sayra's research demonstrated that bioadsorbents derived from avocado peel and seed effectively eliminated RhB dye, with seed achieving a 92% clearance rate at pH 3 after 4 hours [2]. Hoa's work assessed mesoporous carbon (OMC (SBA-15)) for RhB adsorption, revealing a maximum capacity of 400 mg/g, characterized by a pore size of 4.5nm and a surface area of 1,126m^2/g [3]. Advanced oxidation processes (AOPs) have evolved as an efficient treatment technique, facilitating the swift breakdown of organic pollutants by the generation of highly reactive radicals. Piotr's research indicated that the O_3/UV process was the most efficacious for RhB decolorization (90% in 30 minutes at 100mg/L), although the integrated PDS/O_3/UV process demonstrated potential for elevated RhB concentrations [4]. The work by Kambiré et al. demonstrated that the Fenton process effectively oxidized RhB (99.42% at pH 2), with degradation efficiency diminishing in the presence of inorganic ions ($Cl^- < NO_3^- < SO_4^{2-} < PO_4^{3-}$) [5].

Zero-valent iron (Fe^0) has been thoroughly investigated as a useful catalyst in advanced oxidation processes (AOPs) because of its significant reactivity, minimal toxicity, and economic viability [6-8]. The aggregation and passivation of Fe^0 nanoparticles frequently constrain their practical applicability. To address these limitations, Fe^0 is frequently supported on porous substrates, such as activated carbon (AC), which can raise dispersion, augment surface area, and elevate catalytic efficacy [9-11]. Activated carbon, sourced from diverse biomass, is esteemed for its superior adsorption capability and structural integrity, rendering it an optimal support material for catalytic applications [12-14]. In recent years, nano-Fe^0/activated carbon (nZVI/AC) composites have garnered significant interest for wastewater treatment applications [15, 16]. These composites utilize the synergistic effects of Fe^0 nanoparticles and activated carbon, improving the adsorption and catalytic degradation of organic contaminants [17, 18]. The porous composition of activated carbon enables the capture of contaminants. Simultaneously, Fe^0 nanoparticles facilitate degradation via Fenton-like processes, producing reactive oxygen species (ROS) that efficiently decompose intricate dye molecules [19-21]. Green synthesis of nanomaterials using plant extracts offers a sustainable and eco-friendly route, with natural phytochemicals acting as reducing and stabilizing agents. *Terminalia catappa* leaf extract, rich in polyphenols, flavonoids, tannins, and ascorbic acid, was used to reduce Fe^{3+} to zero-valent iron nanoparticles (Fe^0). These compounds also stabilize the nanoparticles by capping their surfaces and preventing agglomeration. The resulting Fe^0/activated carbon composite serves as an efficient catalyst for Rhodamine B degradation, leveraging both the reactivity of Fe^0 and the adsorption capacity of activated carbon. Unlike the biomass-based Fe/AC from *Terminalia catappa* leaves targeting methylene blue removal [22] or the unsupported nZVI used for Bisphenol A adsorption with simulation insights [23], this work focuses on real-time Fenton-like catalytic degradation of a more structurally complex dye. The synergistic interaction between Fe^0 and AC enhances electron transfer, prevents nanoparticle agglomeration, and improves radical generation efficiency. Overall, the study offers a practical and mechanistically distinct approach to treating persistent xanthene dyes.

Comprehending the mechanisms of oxidative degradation of RhB using nZVI/AC composites can yield significant insights for the advancement of effective and sustainable water treatment systems. This research will enhance the field of environmental remediation by showcasing the efficacy of nano-engineered materials in tackling wastewater contamination issues. This study examines the production, characterisation, and catalytic efficacy of nano-Fe^0/activated carbon composites for the oxidative degradation of Rhodamine B dye in aqueous solutions. The main aims are to optimize the synthesis of nZVI/AC composites, evaluate their physicochemical features, and analyze their catalytic efficacy in the degradation of RhB under diverse experimental settings. The research examines the impact of critical operating parameters, including initial dye concentration, and catalyst dosage, on degrading efficiency.

2. MATERIALS AND METHODS

2.1. Preparation of *Terminalia catappa* leaf extract

The extract of *Terminalia catappa* leaves was synthesized by hot water extraction method. Specifically, fresh *Terminalia catappa* leaves were washed, dried at 50 - 60°C and crushed. Then, 5g of dry material was boiled in 100mL of ethanol at 80°C for 60 minutes. The mixture after extraction was filtered through Whatman No.1 filter paper to obtain a clear extract. The obtained extract can be stored in a sealed plastic bottle and used gradually.

2.2. Syntheis of nZVI/AC composite

Measure 6.75g of $FeCl_3{\cdot}6H_2O$ into a flask containing 25mL of distilled water and swirl to achieve thorough homogenization. Employ ultrasonography to confirm complete disintegration. Introduce 0.5g of activated carbon into 50mL of ferric chloride solution and sonicate for 30 minutes. The incremental incorporation of 50mL of *Terminalia catappa* leaf extract while agitating for 2 hours. Allow the mixture to rest overnight. After the overnight period, filter the mixture and purify the resulting component using an distilled water; then, centrifuge at 6000rpm for 20 minutes to obtain the precipitate.

2.3. Characterization of nZVI/AC composite

The infrared (IR) spectra of the material were obtained using an FT-IR spectrometer within the range of 400 - 4000cm^{-1}. Scanning electron microscopy (SEM) was utilized to examine the surface and morphology of the nZVI/AC composite. X-ray diffraction (XRD) patterns of the powder were acquired utilizing a diffractometer with CuKα radiation at 15mA and 40kV.

2.4. Degradation of Rhodamine B

The degradation of Rhodamine B (RhB) utilizing nZVI/AC was performed under regulated laboratory settings to assess the catalytic efficacy of the material. In a standard experiment, a predetermined concentration of RhB solution (often between 2.5 and 15mg/L) was created in a constant volume, typically 100mL. A precise quantity of nZVI/AC catalyst (ranging from 0.05 to 0.30g/L) was subsequently introduced to the solution, and the mixture was agitated at a consistent velocity (about 150 - 200rpm) at ambient temperature. At specified time intervals (0, 10, 20, 30,..., 120 minutes), samples were extracted and promptly filtered or centrifuged to eliminate the solid catalyst. The residual concentration of RhB in the solution was quantified using a UV-Vis spectrophotometer at the peak absorbance wavelength of 553nm. The efficiency of RhB removal on nZVI/AC was calculated by the following equation:

$$H\ \% = \frac{(C_0 - C_t)}{C_0} \times 100\% \quad (1)$$

The first-order kinetic model was employed to simulate experimental data to ascertain the surface photodegradation rate constant:

$$\ln\left(\frac{C_t}{C_0}\right) = -k_1 t \quad (2)$$

The second-order kinetic model was utilized to simulate the elimination kinetics of RhB by nZVI/AC in solution:

$$\frac{1}{C_t} = \frac{1}{C_0} + k_2 t \quad (3)$$

where C_0, C_t (ppm) are concentration of RhB at intial and t moment, respectively; k_1 (min^{-1}) is the pseudo-first-order rate constant; k_2 ($L.(mg.min)^{-1}$) is the pseudo-second-order rate constant.

3. RESULTS AND DISCUSSION

3.1. Characterization of nZVI/AC composite

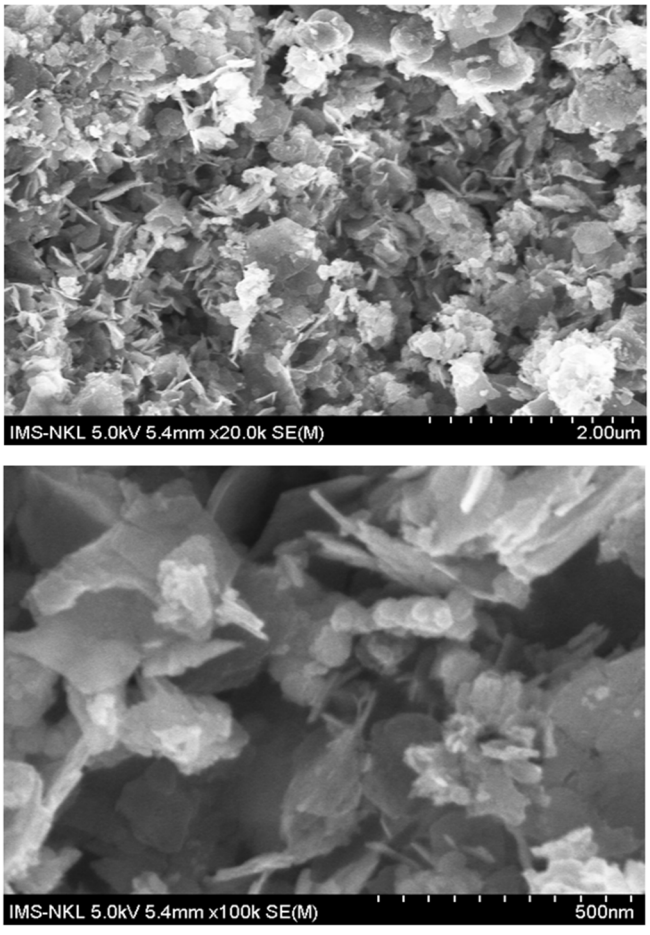

Figure 1. SEM images of nZVI/AC composite

The SEM images in Figure 1 illustrate the morphology of a nZVI/AC composite at various magnifications. The structure has a rough and porous texture, typical of activated carbon. The elevated porosity indicates an

extensive surface area, advantageous for adsorption operations. Nano zero-valent iron particles appear to be distributed throughout the carbon matrix. Some aggregation of nZVI may exist, however accurately assessing particle distribution at this magnification is challenging. This increased magnification exposes the composite's intricate structure. nZVI nanoparticles manifest as diminutive, irregularly shaped aggregates, indicating effective deposition onto the activated carbon surface. The stratified and disjointed appearance of the particles indicates effective dispersion, but with some level of aggregation. The nanoscale characteristics validate the material's capacity for elevated surface reactivity, crucial for adsorption. The porous configuration of activated carbon facilitates harmful absorption by offering multiple active sites. nZVI, recognized for its elevated reactivity, facilitates modification and immobilization. The shape of the composite indicates a synergistic action in which activated carbon facilitates the dispersion of nZVI, hence inhibiting excessive aggregation.

Figure 2 presents the XRD patterns of AC and nZVI/AC composites, offering significant insights into their structural features. The AC sample has a large peak at $2\theta = 20 - 30°$, characteristic of amorphous carbonaceous substances. This broad hump indicates the existence of disordered carbon structures, resembling graphitic domains, however predominantly non-crystalline in nature. The lack of pronounced peaks indicates that the AC does not possess substantial crystalline phases. The nZVI/AC composite retains the broad peak of AC between 20 - 30°, signifying that the carbon structure stays unaltered following nZVI incorporation. Extra diffraction peaks are observed between 44° and 45°, likely corresponding to the (110) plane of α-Fe^0 (bcc iron), so establishing the existence of nano zero-valent iron. The lack of pronounced peaks at 35 - 40° indicates that Fe oxides or hydroxides (Fe_3O_4, Fe_2O_3) are either scarce or exist in an amorphous state. The existence of nZVI in the composite is indicated by the supplementary diffraction characteristics relative to pure AC. The comparatively wide peaks of nZVI signify its nanoscale characteristics, as nanoparticles often exhibit reduced crystallinity and wider diffraction peaks. The AC matrix presumably aids in preventing excessive aggregation of nZVI, hence maintaining its high reactivity. This structure is advantageous for adsorption and reduction processes, especially in heavy metals and toxic organic compounds removal applications.

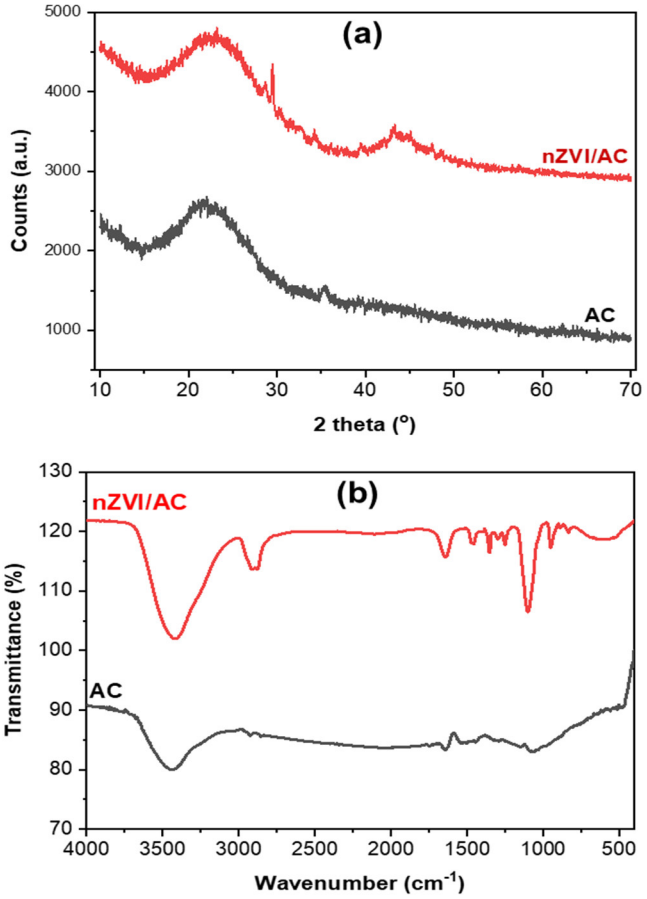

Figure 2. The XRD patterns (a) and FTIR spectroscopy (b) of AC and nZVI/AC composite

Figure 2b displays the Fourier Transform Infrared (FTIR) spectra, comparing the functional groups of activated carbon (AC) with the nZVI/AC composite. The AC spectrum displays distinct peaks corresponding to the functional groups found in activated carbon. The nZVI/AC spectrum displays notable alterations, signifying interactions between nZVI and AC. A prominent peak between 3400 and 3600cm^{-1} in both spectra indicates the stretching vibrations of hydroxyl (-OH) groups, potentially resulting from water adsorption or surface hydroxyl groups. The intensity of this band in the nZVI/AC composite seems diminished, indicating a potential interaction between nZVI and surface hydroxyl groups. Peaks in the 1600 - 1700cm^{-1} range are generally ascribed to C=O stretching in carboxyl or carbonyl moieties and C=C stretching in aromatic rings. In the nZVI/AC spectrum, some peaks exhibit shifts or reductions, suggesting potential reduction or interaction with nZVI. New peaks in the nZVI/AC spectra between 500 - 600 cm^{-1} are attributed to Fe-O vibrations, so proving the existence of iron oxides or hydroxides resulting from the oxidation of nZVI. The bands in the 1000 - 1500cm^{-1} range,

associated with C-O stretching and C-H bending, are altered in nZVI/AC, indicating surface alterations resulting from nZVI integration. The FTIR spectra indicate that the addition of nZVI alters the surface chemistry of AC, resulting in modifications to functional groups. The establishment of Fe-O bonds and modifications in oxygen-containing groups indicate robust interactions between AC and nZVI, potentially augmenting adsorption and reactivity in environmental applications like pollutant removal.

The EDX spectrum of the nZVI/AC composite in Figure 3 indicates the elemental composition of the substance. Carbon (C, 20.86 wt%) is predominantly sourced from the AC support, affirming the function of AC as a substrate for nZVI particles. The elevated oxygen concentration (O, 52.43 wt%) indicates the oxidation of nZVI, resulting in the formation of iron oxides or hydroxides on the surface. This may also be ascribed to oxygen-containing functional groups in activated carbon. Iron (Fe, 9.02 wt%) signifies the existence of nZVI, the active component for adsorption and reduction processes. The chlorine content (6.93 wt%) in the material likely originates from the use of $FeCl_3$ during synthesis, indicating possible surface modification or adsorption of chloride ions. The high content of potassium (6.52 wt%) and calcium (4.24 wt%) originate from the natural composition of the precursor material (coffee husk). The EDX spectrum corroborates the effective synthesis of the nZVI/AC composite, affirming the coexistence of nZVI and AC, along with potential surface oxidation of nZVI. The elemental composition indicates that the composite preserves the fundamental characteristics of both nZVI and AC, rendering it appropriate for environmental applications such pollution adsorption and reduction.

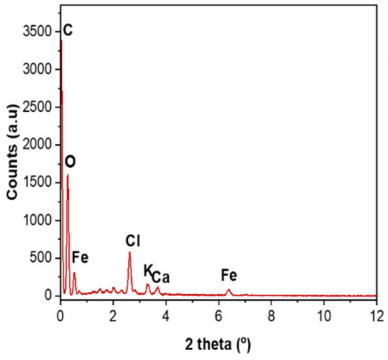

Element	Weight%	Atomic%
O	52.43	72.29
Cl	6.93	5.15
C	20.86	12.98
K	6.52	3.68
Ca	4.24	2.34
Fe	9.02	3.56
Totals	100.00	

Figure 3. The EDX spectra of nZVI/AC composite

3.2. Degradation of Rhodamine B

Figure 4 present the influence of initial RhB concentration and nZVI/AC composite dosage on the degradation efficiency (H%) over time. In Figure 4a, it is evident that increasing the initial RhB concentration from 2.5 to 15.0mg/L leads to a gradual decline in degradation efficiency. At the lowest concentration of 2.5mg/L, the composite achieved nearly 100% degradation within 60 minutes, indicating abundant active sites and minimal resistance to mass transfer. As the concentration rose to 5.0 and 7.5mg/L, the degradation remained effective (above 85%) but with a slightly reduced rate, particularly in the first 40 minutes. For higher concentrations, such as 10.0 - 15.0mg/L, the removal efficiency dropped further, reaching only around 80% at 15.0mg/L after 120 minutes. This decline is likely due to the saturation of active sites on the composite surface, increased competition among RhB molecules, and possible accumulation of degradation intermediates that inhibit further reactions. Figure 4b illustrates the opposite effect with increasing nZVI/AC dosage from 0.05 to 0.30g/L, where a higher dosage enhances the degradation efficiency significantly. At 0.05g/L, only about 70% removal was achieved after 120 minutes, while increasing the dosage to 0.10 and 0.15g/L improved H% to approximately 80 - 90%. Further increases in dosage to 0.20, 0.25, and 0.30g/L led to a plateauing effect, where the degradation reached near-complete levels (> 90%) within 80 minutes. This improvement is attributed to the greater number of reactive sites and Fe^0 content available for redox reactions and adsorption. However, the marginal difference between 0.20 and 0.30g/L suggests that excessive dosage may not proportionally enhance the degradation, possibly due to particle agglomeration or limited pollutant availability relative to the active sites. Together, these results emphasize that while lower initial dye concentrations and higher nZVI/AC dosages favor efficient RhB degradation, there exists an optimal range beyond which performance gains become minimal due to site saturation or other limiting factors.

Figure 5 illustrates the degrading efficiency of RhB over time utilizing nZVI/AC. The concentration of RhB (Ct) declines markedly within the initial 30 to 60 minutes. Following 60 minutes, the degradation rate diminishes, with Ct attaining a minimal value of 0.93603mg/L at 120 minutes. This pattern indicates that the reaction adheres to a pseudo-first-order kinetic model, wherein the first rapid degradation phase is associated with an increased availability of active sites and reactive species. The deterioration efficiency H rapidly improves, attaining 90.52% at 120 minutes. A fast escalation is noted within the initial 60 minutes, attaining 81.28% degradation,

signifying substantial efficiency in the preliminary phases. After 60 minutes, the efficiency curve stabilizes, indicating a deceleration of the process attributed to diminished availability of RhB molecules and possible surface saturation effects. The elevated clearance rate within the initial 60 minutes signifies that nZVI/AC is exceptionally efficient in RhB adsorption and degradation during the preliminary phases. As the reaction advances, the degradation diminishes owing to a reduction in accessible RhB molecules and potential deactivation of active sites. The degradation efficiency over 90% illustrates the efficacy of nZVI/AC in removing RhB. The degrading effectiveness of RhB utilizing nZVI/AC is contingent upon time, exhibiting fast elimination during the initial hour. Beyond this juncture, the reaction decelerates however persists in efficiently eliminating RhB, attaining over 90% degradation after 120 minutes. This indicates that nZVI/AC is an exceptionally efficient material for the therapy of RhB, especially within brief reaction periods.

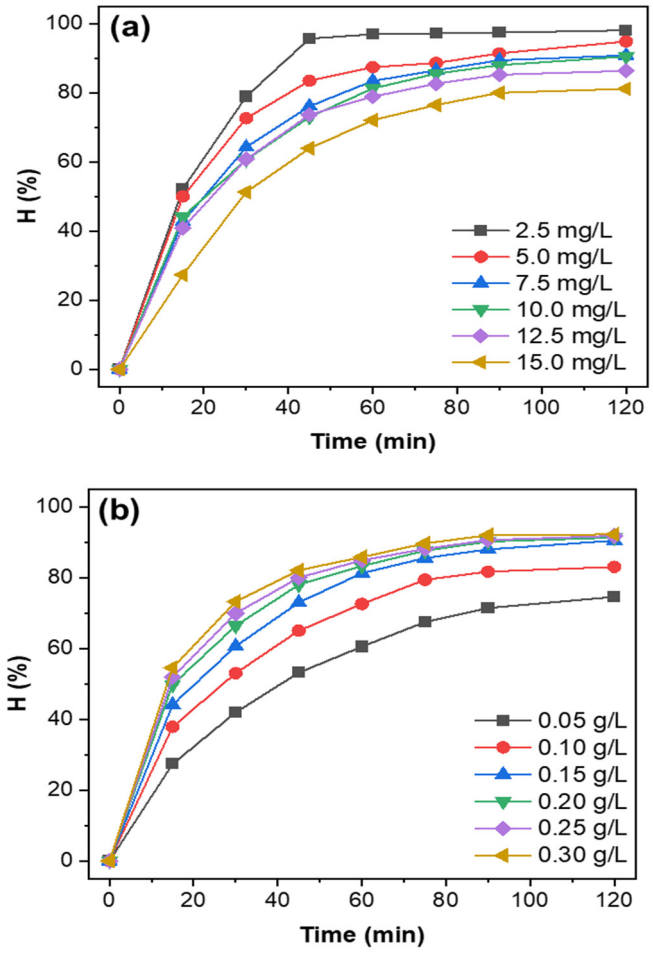

Figure 4. Effect of initial concentration (a) and dosage (b) on degradation effeciency of RhB vs time with nZVI/AC composite

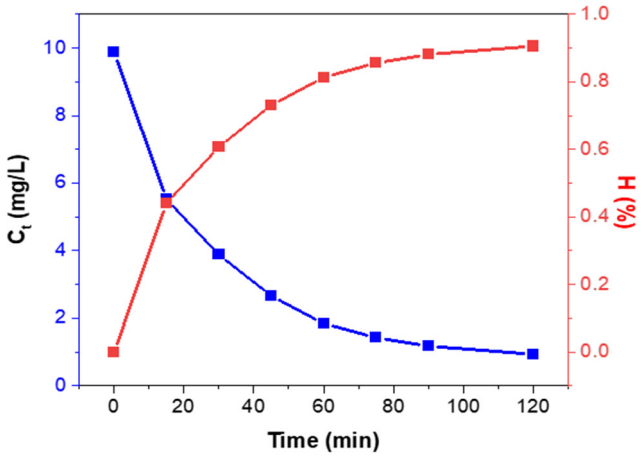

Figure 5. The degradation efficiency of RhB vs irradiation time with nZVI/AC

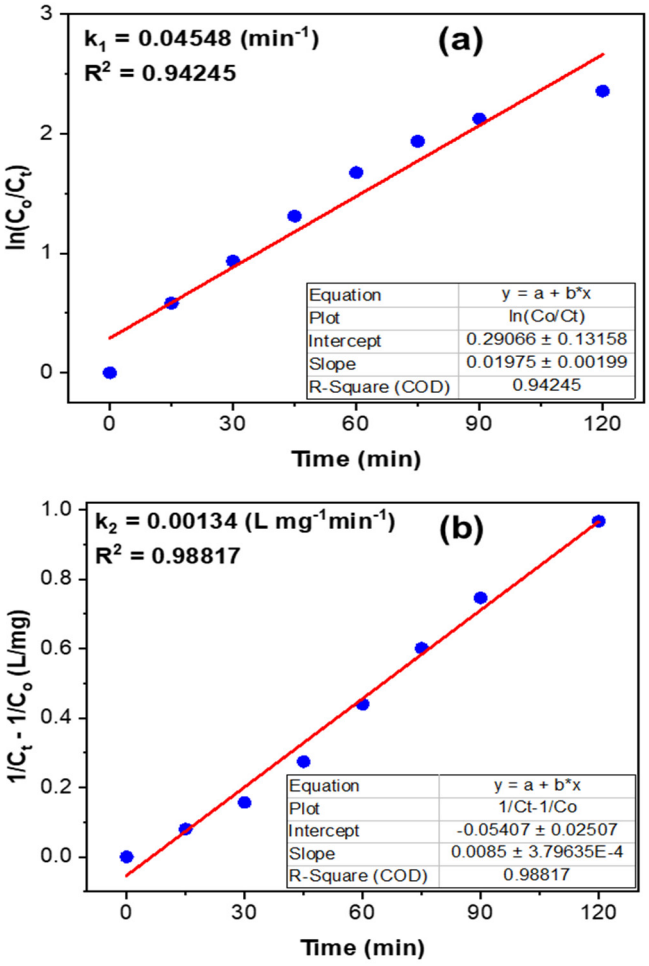

Figure 6. The first-pseudo order (left) and second-pseudo order (right) models of RhB degradation on nZVI/AC

Figure 6 displays the kinetic modeling of RhB degradation with nZVI/AC, contrasting pseudo-first-order (Figure 6a) and pseudo-second-order (Figure 6b) reaction models. In the pseudo-first-order model, the rate constant is k_1 = 0.04548min^{-1}. The coefficient of

determination is R^2 = 0.94245, signifying a reasonably good fit with significant discrepancies. This model indicates that the degradation rate is contingent upon the concentration of RhB, adhering to an exponential decay pattern. The pseudo-second-order rate constant is k_2 = 0.00134L.mg^{-1}.min^{-1}. The coefficient of determination (R^2 = 0.98817) exceeds that of the first-order model, signifying a superior fit. This indicates that the degradation rate is affected by both RhB concentration and the accessible reactive sites on nZVI/AC. The elevated R^2 value in the pseudo-second-order model indicates that it more accurately characterizes the RhB degrading process. This suggests that adsorption and surface contacts are crucial in the elimination of RhB, rather than solely relying on concentration-based degradation. The pseudo-second-order model suggests that the reaction may be governed by chemical adsorption (chemisorption) instead of mere mass transfer. The degradation of RhB by nZVI/AC adheres more closely to a pseudo-second-order kinetic model than to a pseudo-first-order one. This indicates that the reaction is governed by surface dynamics, possibly involving chemisorption or surface contacts, rather than being solely reliant on RhB concentration in solution.

4. CONCLUSION

This work nZVI, recognized for its high reactivity, enables modification and immobilization. The AC matrix likely assists in inhibiting the excessive aggregation of nZVI, hence preserving its elevated reactivity. The FTIR spectra demonstrate that the incorporation of nZVI modifies the surface chemistry of AC, leading to changes in functional groups. The elemental composition indicates that the composite preserves the fundamental characteristics of both nZVI and AC, rendering it appropriate for environmental applications such pollution adsorption and reduction. The study investigated the degradation of Rhodamine B (RhB) using nZVI/AC under several conditions, including variable initial concentrations, catalyst dosages, and reaction times. The degradation process adhered to pseudo-second-order kinetics (R^2 = 0.988), signifying that the reaction was dictated by adsorption and surface contacts rather than mere mass transfer. The pseudo-first-order model yielded a satisfactory fit but exhibited a diminished correlation (R^2 = 0.942), further indicating that chemisorption was the predominant mechanism. RhB degradation transpired swiftly within the initial 60 minutes, exceeding 80% elimination, and progressed at a diminished rate, with a peak efficiency of 90.52% after 120 minutes. This illustrates the significant efficacy of nZVI/AC for the treatment of RhB in aqueous solutions. The findings validate that nZVI/AC is an exceptionally effective substance for the breakdown of RhB, positioning it as a viable option for wastewater treatment applications.

ACKNOWLEDGEMENT

This research was financed by the National Foundation for Science and Technology Development under grant code NCUD.01-2024.15 and conducted at the Joint Vietnam-Russia Tropical Science and Technology Research Center.

REFERENCES

[1]. Yang S., Feng Y., Liu N., Zhao Y., Wang X., Zhang Z., Chen H., Yu Y., "Enhancement on the removal of Rhodamine B (RhB) by means of the Enlarged Anode Electric Biological (EAEB) reactor," *Chemosphere,* 245, 125566, 2020.

[2]. Orozco S., Montiel E., Valencia J. E., González R. G., del Carmen Chávez Parga M., Cortés J. A., Rivero M., "Effective RhB dye removal using sustainable natural bioadsorbents synthesized from avocado seed and skin," *Water, Air, & Soil Pollution*, 235, 155, 2024.

[3]. El-Shafey S. S., Ahmed S. A. S., Aboelenin R. M., Fathy N. A., "Synthesis of SBA-16 mesoporous silica from rice husk ash for removal of Rhodamine B cationic dye: Effect of hydrothermal treatment time," *Desalination and Water Treatment*, 317, 100179, 2024.

[4]. Zawadzki P., Deska M., "Degradation efficiency and kinetics analysis of an advanced oxidation process utilizing ozone, hydrogen peroxide and persulfate to degrade the dye rhodamine B," *Catalysts*, 11, 974, 2021.

[5]. Ollo K., Abollé A., Rodrigue K. A., Eudoxie K. A., Sylvestre K. K., Etienne K. K., Jocelin K. K., Souleymane K., Lassiné O., "Oxidation of rhodamine B using the Fenton process: optimization, kinetics and inorganic ions studies," *Journal de la Société Ouest-Africaine de Chimie*, 51, 2022.

[6]. Liu M., Ye Y., Xu L., Gao T., Zhong A., Song Z., "Recent advances in nanoscale zero-valent iron (nZVI)-based advanced oxidation processes (AOPs): Applications, mechanisms, and future prospects," *Nanomaterials*, 13, 2830, 2023.

[7]. Bajagain R., Jeong S. W., "Degradation of petroleum hydrocarbons in soil via advanced oxidation process using peroxymonosulfate activated by nanoscale zero-valent iron," *Chemosphere*, 270, 128627, 2021.

[8]. Mends A., Pirgalıoğlu S., "Advanced Oxidation of Dye Solutions with Persulfate Activated by Zero Valent Iron," In *International Conference on Water Problems in Mediterranean Countries*, 411-419, Springer, 2023.

[9]. Mortazavian S., An H., Chun D., Moon J., "Activated carbon impregnated by zero-valent iron nanoparticles (AC/nZVI) optimized for simultaneous adsorption and reduction of aqueous hexavalent chromium: Material characterizations and kinetic studies," *Chemical Engineering Journal*, 353, 781-795, 2018.

[10]. Xu Y., Liu Z., Ma K., Qin Q., "Facile synthesis of high iron content activated carbon-supported nanoscale zero-valent iron for enhanced Cr (VI) removal in aqueous solution," *Chemosphere,* 291, 132709, 2022.

[11]. An L., Xiao P., "Zero-valent iron/activated carbon microelectrolysis to activate peroxydisulfate for efficient degradation of chlortetracycline in aqueous solution," *Rsc Advances*, 10, 19401-19409, 2020.

[12]. Malini K., Selvakumar D., Kumar N., "Activated carbon from biomass: Preparation, factors improving basicity and surface properties for enhanced CO_2 capture capacity - A review," *Journal of CO_2 Utilization,* 67, 102318, 2023.

[13]. Gan Y., "Activated carbon from biomass sustainable sources," *C*, 7 (2): 39, 2021.

[14]. Volperts A., Plavniece A., Dobele G., Zhurinsh A., Kruusenberg I., Kaare K., Locs J., Tamasauskaite-Tamasiunaite L., Norkus E., "Biomass based activated carbons for fuel cells," *Renewable Energy*, 141, 40-45, 2019.

[15]. Su H., Dou X., Xu D., Feng L., Liu Y., Du Z., Zhang L., "Fe0-loaded superfine powdered activated carbon prepared by ball milling for synergistic adsorption and persulfate activation to remove aqueous carbamazepine," *Chemosphere*, 293, 133665, 2022.

[16]. Okonji S. O., Yu L., Dominic J. A., Pernitsky D., Achari G., "Adsorption by granular activated carbon and nano zerovalent iron from wastewater: A study on removal of selenomethionine and selenocysteine," *Water*, 13, 23, 2020.

[17]. Raji M., Mirbagheri S. A., Ye F., Dutta J., "Nano zero-valent iron on activated carbon cloth support as Fenton-like catalyst for efficient color and COD removal from melanoidin wastewater," *Chemosphere,* 263, 127945, 2021.

[18]. Almujaybil M. J., Abunaser D. F. M., Gouda M., Khalaf M. M., Mohamed I. M., Abd El-Lateef H. M., "Facile synthesis of Fe (0)@ activated carbon material as an active adsorbent towards the removal of Cr (VI) from aqueous media," *Catalysts,* 12, 515, 2022.

[19]. Suryawanshi P. L., Upadhyay P., Bethi B., Moholkar V. S., Chakma S., "Fenton with zero-valent iron nanoparticles (nZVI) processes: Role of nanomaterials," In *Handbook of Nanomaterials for Wastewater Treatment*, 847-866, Elsevier, 2021.

[20]. Taha M., Ibrahim A., Amat R., Azhari A., "Applicability of nano zero valent iron (nZVI) in sono-Fenton process," *Journal of Physics: Conference Series*, p 012010, IOP Publishing, 2014.

[21]. Li D., Fu Y., Hong W., Li S., Qiu M., Yu H., Wang H., Wu J., Yang Q., Yang S.,, "Customizable three-dimensional printed zerovalent iron: An efficient and reusable Fenton-like reagent for florfenicol degradation," *Environmental Science & Technology*, 58, 19501-19513, 2024.

[22]. Nguyen N. T. K., Le D. T. T., Vo K. D., Huynh L. T., Nguyen H. M., Tran-Thuy T. M., Nguyen L. Q., Van Nguyen D., "Valorization of tropical almond (*Terminalia catappa*) leaves into iron-containing activated carbon for rapid catalytic degradation of methylene blue with hydrogen peroxide," *J. Ecol. Eng.*, 25(8):54-61, 2024.

[23]. Sulaiman W. K., Azeez L., Adebisi S. A., Wahab O. O., Agbaogun B. K., "Exploring zero-valent iron nanoparticles (nZVI) for Bisphenol A removal: Experimental investigations and Monte-Carlo simulation insights," *Water Practice and Technology*, 19 (8): 3416–3438. 19, 3416-3438, 2024.

THÔNG TIN TÁC GIẢ

Vũ Minh Châu[1], Nguyễn Thị Phượng[2], Vương Thùy Trang[3], Nguyễn Bá Cường[4], Nguyễn Thị Hồng Phượng[3], Nguyễn Thị Hoài Phương[1]

[1]Trung tâm Nhiệt đới Việt - Nga

[2]Viện Hóa học - Vật liệu, Viện Khoa học và Công nghệ Quân sự

[3]Đại học Bách khoa Hà Nội

[4]Học viện Kỹ thuật Quân sự